

An Optimal Control Approach to Flocking

Logan E. Beaver, *Student Member, IEEE*, Chris Kroninger, Andreas A. Malikopoulos, *Senior member, IEEE*

Abstract—Large-scale flocking behavior has been an area of significant research in multi-agent systems and control. To date, the structure of flocking has been predominantly studied through the application of artificial potential fields coupled with velocity consensus. These approaches do not consider the energy cost of the agents during flocking, which is especially important in large-scale robot swarms. This work introduces an optimal control framework to induce flocking in a group of agents. Guarantees of energy minimization and safety are provided, along with a decentralized algorithm which satisfies the derived optimality conditions and is realizable in real time. The efficacy of the proposed control algorithm is evaluated through simulation in both MATLAB and Gazebo.

I. INTRODUCTION

A. Background

Complex systems consist of many interdependent, independent agents which are connected to each other in both space and time [1]. The individual interactions between agents may result in unpredictable emergent behavior at a large scale. As the world becomes increasingly complex [2] modern control approaches will be required to optimize individual agents with an eye on overall system behavior [3], [4].

Multi-agent systems have attracted considerable attention in many applications due to their natural parallelization, general adaptability, and ability to self-organize [5]. This has proven useful in many applications, such as transportation [6], construction [7], and surveillance [8]. Controlling emergent flocking behavior has been of particular interest to robotics researchers since the seminal paper by Reynolds [9], which introduced three heuristic rules for flocking in digital animation: move toward neighboring flockmates, avoid collisions, and match velocity with neighbors. Flocking has many practical applications, such as mobile sensing networks, coordinated delivery, reconnaissance, and surveillance [10].

However, fielding large robot swarms imposes significant cost constraints on each individual. These constraints limit each agent's computational and sensing ability and reduce their individual energy storage capacity. This is the driving force behind energy-optimal control algorithms, which are necessary to extend the useful life of each agent. Currently, the most popular approach to impose flocking in multi-agent systems is the use of artificial potential fields and velocity consensus [11]–[13]. In these approaches, flock aggregation

and collision avoidance are both handled by the potential field, the design of which is still an open question [14]. Several rigorous theoretical guarantees have been proven for these types of flocking models [15]; however, minimum-energy flocking still remains relatively unexplored.

The most significant drawback of potential field methods is that the resulting trajectories are sub-optimal from an energy perspective. This was explicitly stated by Reynolds, who observed that potential fields tend to apply forces perpendicular to flock and agent motion [9]. Several modern approaches have proposed alternative strategies to avoid inter-agent collisions, such as reactive obstacle avoidance [16], dynamic state constraints [17]–[19], initial system constraints [20], and ordered/sequential trajectory planning [21].

B. Contributions of This Paper

In this paper we propose an extension to our previous work on energy-optimal trajectories for formations [22] and apply it to the problem of flocking. This work has three major contributions:

- A continuous decentralized optimal control framework for minimum-energy flocking.
- A closed-form solution for the energy-minimizing control input in the centralized case.
- An adaptation of the centralized optimal solution to the decentralized case.

The proposed framework is related to the robot ecology paradigm for long-duration autonomy [23]. However, this framework achieves optimal behavior using model predictive control to minimize an endpoint cost rather than gradient flow to satisfy a task constraint.

Quitero et al. [24] applied dynamic programming to create an aggregate of fixed-wing aircraft around a leader. In contrast, our work is leaderless and gives explicit safety guarantees. Zhang et al. [25] applied optimal control over a discretized horizon to push agents into a rigid, stable lattice while penalizing energy consumption. Our approach is continuous, has an analytical solution, and allows flexibility in the flock shape. Gomez et al. [26] used a centralized controller to derive optimal trajectories for teams of agents to flock. Our approach adapts the centralized solution to a decentralized system and therefore does not require a central computer to plan trajectories. Finally, Hu et al. [27] introduced a discretized model predictive control framework to minimize energy consumption, avoid collisions, and reduce communication via self-triggered updates. Our work provides an analytical solution to the continuous form of this problem, reducing the computational burden on each agent and allowing our algorithm to be executed in real time.

This research was supported by Combat Capabilities Development Command, Army Research Laboratory, MD, USA.

Logan and Andreas are with the Department of Mechanical Engineering, University of Delaware, Newark, DE 19711, USA

Chris is with Combat Capabilities Development Command, Army Research Laboratory, MD, USA.

C. Organization of this Paper

The remainder of the paper is structured as follows. We formulate the problem in Section II and state the assumptions of our approach. In Section III, we solve the optimization problem for the unconstrained and constrained cases and give an analytical function for the resulting controller. In Section IV, we provide two sets of simulation results and discuss the observed emergent behavior. In the first set, we use MATLAB to demonstrate the viability of the proposed control scheme; in the second set, we use Gazebo to validate a minimum-communication approach, which reformulates the control method to use pure sensing. Finally, we draw conclusions and discuss future work in Section V.

II. PROBLEM FORMULATION

Consider a flock of $N \in \mathbb{N}$ agents indexed by the set $\mathcal{A} = \{1, 2, \dots, N\}$. Each agent $i \in \mathcal{A}$ follows the double integrator dynamics,

$$\dot{\mathbf{p}}_i(t) = \mathbf{v}_i(t), \quad (1)$$

$$\dot{\mathbf{v}}_i(t) = \mathbf{u}_i(t), \quad (2)$$

where $t \in \mathbb{R}_{\geq 0}$ is the time, and $\mathbf{p}_i(t), \mathbf{v}_i(t), \mathbf{u}_i(t) \in \mathbb{R}^2$ are the position, velocity, and control input, respectively. Each agent occupies a closed disk of radius $R \in \mathbb{R}_{>0}$. The state of each agent is given by

$$\mathbf{x}_i(t) = \begin{bmatrix} \mathbf{p}_i(t) \\ \mathbf{v}_i(t) \end{bmatrix}. \quad (3)$$

The speed and control input are constrained by an upper and lower limit such that

$$v_i^{\min} \leq \|\mathbf{v}_i\| \leq v_i^{\max}, \quad (4)$$

$$u_i^{\min} \leq \|\mathbf{u}_i\| \leq u_i^{\max}. \quad (5)$$

For any pair of agents $i, j \in \mathcal{A}$, the relative displacement between them is described by the vector

$$\mathbf{s}_{ij}(t) = \mathbf{p}_j(t) - \mathbf{p}_i(t), \quad i, j \in \mathcal{A}. \quad (6)$$

To guarantee safety within the system, we impose the following constraints:

$$\mathbf{s}_{ij}(t) \cdot \mathbf{s}_{ij}(t) \geq 4R^2 \quad \forall t \in \mathbb{R}_{>0}, \quad (7)$$

$$h > 2R, \quad (8)$$

where (7) guarantees collision avoidance and (8) is a system-level constraint which allows collisions to be detected before they occur. The squared form of (7) is selected as its derivative with respect to $\mathbf{p}_{ij}(t)$ is smooth, which will simplify the analytical solution presented in Section III.

Each agent has also a sensing/communicating distance, $h \in \mathbb{R}_{>0}$, which is used to define its neighborhood.

Definition 1. The *neighborhood* of each agent $i \in \mathcal{A}$, is defined by the set

$$\mathcal{N}_i(t) = \{j \in \mathcal{A} \mid \|\mathbf{s}_{ij}(t)\| < h\}, \quad (9)$$

where $\|\cdot\|$ is the Euclidean norm.

The neighborhood is allowed to switch over time, and $i \in \mathcal{N}_i(t)$ always. Agent i is able to communicate with any agent $j \in \mathcal{N}_i$ and sense its current state, $\mathbf{x}_j(t)$. A schematic of the system is presented in Figure 1.

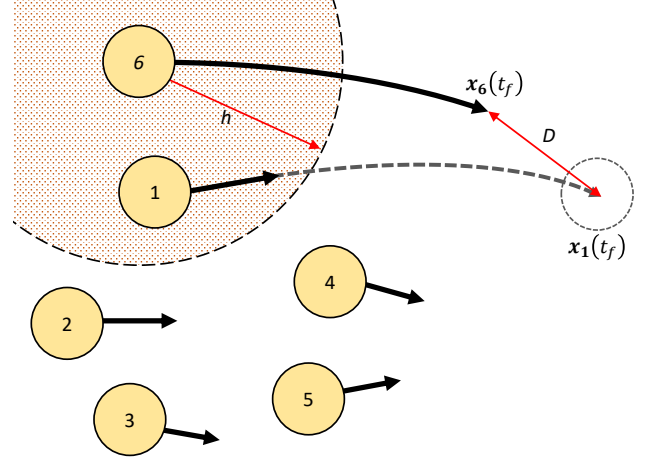


Fig. 1. A diagram of 6 agents flocking. Agent 6 uses the predicted trajectory of all agents in its neighborhood to generate an optimal trajectory which maintains the structure of the flock.

Finally, every agent is also equipped with a long-range sensor which can estimate the centroid of the flock, which is given by

$$\mathbf{p}_{cg}(t) = \frac{1}{N} \sum_{i \in \mathcal{A}} \mathbf{p}_i(t). \quad (10)$$

The purpose of (10) is to drive isolated agents back toward the flock. This can reasonably be achieved with inexpensive audio or visual sensors in the case where a majority of the agents have already formed an aggregate. However, for the case where there is no clear flock, it may be challenging to determine (10) in practice.

Each agent $i \in \mathcal{A}$ generates a trajectory for a given time interval $t \in [t_0, t_f]$, where $t_f - t_0 > 0$ is the horizon. Agent i then follows this generated trajectory for some period ΔT , at which point the trajectory is recalculated over the new interval $t \in [t_0 + \Delta T, t_f + \Delta T]$. The trajectory generated by agent $i \in \mathcal{A}$ is the outcome of minimizing the flocking error function, which we define next.

Definition 2. For all agents $i \in \mathcal{A}$, the *flocking error* is defined by the scalar function

$$\Phi(\mathbf{x}_i, t_f) = w_1 \phi_d(\mathbf{x}_i, t_f) + w_2 \phi_v(\mathbf{x}_i, t_f) + w_3 \phi_a(\mathbf{x}_i, t_f), \quad (11)$$

$$\phi_d(\mathbf{x}_i, t_f) = \|\mathbf{v}_i(t_f) - \mathbf{v}_d(t_f)\|^2, \quad (12)$$

$$\phi_v(\mathbf{x}_i, t_f) = \|\mathbf{v}_i(t_f) - \mathbf{v}_{\text{avg}}(t_f)\|^2, \quad (13)$$

$$\phi_a(\mathbf{x}_i, t_f) = \begin{cases} (\|\mathbf{p}_{cg}(t_f) - \mathbf{p}_i(t_f)\| - D)^2, & |\mathcal{N}_i(t_0)| = 1 \\ \sum_{j \in \mathcal{N}_i(t_0)} (\mathbf{s}_{ij}(t_f) \cdot \hat{\mathbf{p}}_{ij}(t_f) - D)^2, & |\mathcal{N}_i(t_0)| > 1 \end{cases} \quad (14)$$

where w_1, w_2 , and w_3 are normalizing parameters which weight the influence of velocity control $\phi_d(\mathbf{x}_i, t_f)$, velocity matching $\phi_v(\mathbf{x}_i, t_f)$, and aggregation $\phi_a(\mathbf{x}_i, t_f)$ in the overall system behavior. The symbol $|\cdot|$ denotes set cardinality while the system parameters $\mathbf{v}_d(t_f)$ and D set the desired flock velocity and separating distance between agents. The average agent speed, $\mathbf{v}_{\text{avg}}(t_f)$, is given by

$$\mathbf{v}_{\text{avg}}(t_f) = \begin{cases} \dot{\mathbf{p}}_{cg}(t_f), & |\mathcal{N}_i(t_0)| = 1, \\ \frac{1}{|\mathcal{N}_i(t_0)|} \sum_{j \in \mathcal{N}_i(t_0)} \mathbf{v}_j(t_f), & |\mathcal{N}_i(t_0)| > 1. \end{cases} \quad (15)$$

The cases in (14) and (15) are equivalent to placing a virtual agent at the centroid of the flock for any agent which becomes isolated. This ensures that any isolated agents will return to the flock.

Each agent generates its energy-optimal trajectory by solving the following optimal control problem.

Problem 1. (*Minimum-energy flocking*)

For every agent $i \in \mathcal{A}$,

$$\min_{\mathbf{u}_i(t)} \left\{ \Phi(\mathbf{x}_i, t_f) + \int_{t_0}^{t_f} \|\mathbf{u}_i(t)\|^2 dt \right\} \quad (16)$$

subject to: (1), (2), (4), (5), (7), $\mathbf{x}_i(t_0) = \mathbf{x}_i^0$,

where $\Phi(\mathbf{x}_i, t_f)$ is given by Definition 2 and \mathbf{x}_i^0 is the initial state of agent i .

By minimizing the L^2 norm of the control input (acceleration) we expect to see a proportional reduction in energy consumption. To solve Problem 1, we impose the following assumptions.

Assumption 1. There are no external disturbances or obstacles.

Assumption 1 is imposed to evaluate the idealized performance of the proposed algorithm. It is well known that optimal control can be sensitive with respect to noise and disturbances, and this assumption may be relaxed by introducing a measure of robustness into Problem 1.

Assumption 2. There are no errors or delays with respect to communication and sensing.

The strength of Assumption 2 is application dependent. In general, it has been shown that sparse updates to model predictive control are sufficient [27]. However, these delays may become significant for large or fast-moving swarms in constrained environments.

Assumption 3. The flock is low-density (only two agents ever come within distance $s = 2R$ of each other).

Assumption 3 may be a strong assumption; however, Assumption 1 and the energy-minimizing nature of the system tend to naturally avoid collisions between agents for reasonable initial conditions, i.e., $\mathbf{s}_{ij}(t_0) > D$, $i, j \in \mathcal{A}, j \neq i$. This assumption is only required to simplify the analytical solution, and it may be relaxed given that each agent has sufficient computational abilities to solve the resulting boundary value problem for a multi-agent interaction.

III. SOLUTION METHODOLOGY

To derive an analytical solution for Problem 1 we use Hamiltonian Analysis [28]. As the case where the state and control constraints, (4) and (5), are active is well studied in the literature [6] we will only consider the case where they are finite but never become active.

As a first step the constraint (7) must be derived until the control input $\mathbf{u}_i(t)$ appears,

$$\mathbf{N}_i(t) = \begin{bmatrix} 4R^2 - \mathbf{s}_{ij}(t) \cdot \mathbf{s}_{ij}(t) \\ -\mathbf{s}_{ij}(t) \cdot \dot{\mathbf{s}}_{ij}(t) \\ -\mathbf{s}_{ij}(t) \cdot \ddot{\mathbf{s}}_{ij}(t) - \dot{\mathbf{s}}_{ij}(t) \cdot \dot{\mathbf{s}}_{ij}(t) \end{bmatrix} \leq \mathbf{0}. \quad (17)$$

The Hamiltonian is then augmented by the final row of $\mathbf{N}_i(t)$ to form the control Hamiltonian,

$$H_i = \|\mathbf{u}_i(t)\|^2 + \boldsymbol{\lambda}_i^p(t) \cdot \mathbf{v}_i(t) + \boldsymbol{\lambda}_i^v(t) \cdot \mathbf{u}_i(t) - \sum_{j \in \mathcal{N}_i} \mu_{ij}(t) \left(\mathbf{s}_{ij}(t) \cdot \ddot{\mathbf{s}}_{ij}(t) + \dot{\mathbf{s}}_{ij}(t) \cdot \dot{\mathbf{s}}_{ij}(t) \right) \quad (18)$$

where $\boldsymbol{\lambda}_i^p(t), \boldsymbol{\lambda}_i^v(t)$ are the position and velocity covectors, and $\mu_{ij}(t)$ is an inequality Lagrange multiplier with values

$$\mu_{ij}(t) = \begin{cases} \geq 0 & \text{if } \mathbf{s}_{ij}(t) \cdot \ddot{\mathbf{s}}_{ij}(t) + \dot{\mathbf{s}}_{ij}(t) \cdot \dot{\mathbf{s}}_{ij}(t) = 0, \\ 0 & \text{if } \mathbf{s}_{ij}(t) \cdot \ddot{\mathbf{s}}_{ij}(t) + \dot{\mathbf{s}}_{ij}(t) \cdot \dot{\mathbf{s}}_{ij}(t) < 0. \end{cases} \quad (19)$$

To solve (18) for agent $i \in \mathcal{A}$, we will consider both cases

- i) all agents $j \in \mathcal{N}_i(t)$ satisfy $\mu_{i,j} = 0$,
- ii) any agent $j \in \mathcal{N}_i(t)$ satisfies $\mu_{i,j} > 0$,

and piece the constrained and unconstrained arcs together to arrive at a piecewise-continuous, energy-optimal trajectory. Next, we present the unconstrained motion and boundary conditions followed by the decentralized algorithm for constructing an energy-optimal trajectory in real time.

A. Unconstrained Motion

The energy-optimal unconstrained trajectories for the position, speed, acceleration, and covectors resulting from (18) [6] are

$$\mathbf{p}_i(t) = \frac{1}{6} \mathbf{a}_i t^3 + \frac{1}{2} \mathbf{b}_i t + \mathbf{c}_i t + \mathbf{d}_i, \quad t \in [t_0, t_f] \quad (20)$$

$$\mathbf{v}_i(t) = \frac{1}{2} \mathbf{a}_i t^2 + \mathbf{b}_i t + \mathbf{c}_i, \quad t \in [t_0, t_f] \quad (21)$$

$$\mathbf{u}_i(t) = \mathbf{a}_i t + \mathbf{b}_i, \quad t \in [t_0, t_f] \quad (22)$$

$$\boldsymbol{\lambda}_i^p(t) = \mathbf{a}_i, \quad t \in [t_0, t_f] \quad (23)$$

$$\boldsymbol{\lambda}_i^v(t) = -\mathbf{a}_i t - \mathbf{b}_i \quad t \in [t_0, t_f] \quad (24)$$

where $\mathbf{a}_i, \mathbf{b}_i, \mathbf{c}_i, \mathbf{d}_i \in \mathbb{R}^2$ are constants of integration. Equations (20) - (24) contain 8 unknowns, which are solved using 8 boundary conditions;

$$\mathbf{x}_i(t_0) = \mathbf{x}_i^0, \quad (25)$$

$$\boldsymbol{\lambda}_i(t_f) = \frac{\Phi(\mathbf{x}_i, t)}{\mathbf{x}_i} \Big|_{t_f}. \quad (26)$$

Solving (26) yields

$$\lambda_i^p(t_f) = -2w_3 \sum_{j \in \mathcal{N}_i(t_0)} \left((\|\mathbf{s}_{ij}(t_f)\| - D) \mathbf{s}_{ij}(t_f) \right), \quad (27)$$

$$\lambda_i^v(t_f) = 2w_2 \left(\mathbf{v}_i(t_f) - \mathbf{v}_{\text{avg}} \right) + 2w_1 \left(\mathbf{v}_i(t_f) - \mathbf{v}_d \right). \quad (28)$$

We then substitute (6), (23), and (24) into (27) and (28) to solve for $\mathbf{p}_i(t_f)$ and $\mathbf{u}_i(t_f)$. This yields two equations

$$\mathbf{p}_i(t_f) = \frac{\mathbf{a}_i}{2w_3 \sum_j (\|\mathbf{s}_{ij}(t_f)\| - D)} + \sum_{j \in \mathcal{N}_i} \mathbf{p}_j(t_f) \quad (29)$$

$$\mathbf{u}_i(t_f) = -2w_2 \left(\mathbf{v}_i(t_f) - \mathbf{v}_{\text{avg}} \right) - 2w_1 \left(\mathbf{v}_i(t_f) - \mathbf{v}_d \right) \quad (30)$$

where $\mathbf{a}_i = 0$ if the right-hand side of (27) is ever zero.

Equations (25), (26), and (30) give three conditions to solve for the constants \mathbf{b}_i , \mathbf{c}_i , and \mathbf{d}_i in (20) - (24). The value of \mathbf{a}_i can then be found by the solution of (29), which is trivial to compute numerically in real time.

B. Constrained Motion

For any agent $i \in \mathcal{A}$, let the set \mathcal{V}_i be defined as

$$\mathcal{V}_i(t) := \{j \in \mathcal{N}_i(t) \mid \mu_{ij}(t) > 0, j \neq i\}. \quad (31)$$

Thus, when $\mathcal{V}_i \neq \emptyset$ agent i must follow a safety-constrained trajectory. Application of the Euler-Lagrange equations [28] yields

$$u_i(t) = -\lambda_i^v(t) - \sum \mu_{ij}(t) \mathbf{s}_{ij}(t) \quad (32)$$

$$-\dot{\lambda}_i^v(t) = \lambda_i^p(t) + \sum \mu_{ij}(t) \dot{\mathbf{s}}_{ij}(t) \quad (33)$$

$$-\dot{\lambda}_i^p(t) = \sum \mu_{ij}(t) \ddot{\mathbf{s}}_{ij}(t) \quad (34)$$

$$\begin{aligned} \mu_{ij}(t) &= \left(\lambda_j(t) - \lambda_i(t) \right) \mathbf{s}_{ij}(t) - \|\dot{\mathbf{s}}_{ij}(t)\|^2 \\ &\quad + \sum_{k \in \mathcal{V}_j(t), k \neq i} \mu_{jk}(t) \mathbf{s}_{jk}(t) \\ &\quad + \sum_{k \in \mathcal{V}_i(t), k \neq j} \mu_{ik}(t) \mathbf{s}_{ik}(t) \end{aligned} \quad (35)$$

which, in general, must be solved numerically. However, under Assumption 3 we may consider the case where only two agents interact. For the two agent case, we can define the quantity

$$a_{ij}(t) := \|\dot{\mathbf{s}}_{ij}(t)\|. \quad (36)$$

which is the relative speed at which two constrained agents orbit each other. We may then construct a new basis for \mathbb{R}^2 which we define next.

Definition 3. The orthonormal *contact basis* for any two agents in contact, $i \in \mathcal{A}$, $j \in \mathcal{V}_i$, with a nonzero relative speed, is defined as

$$\hat{p}_{ij}(t) := \frac{\mathbf{s}_{ij}(t)}{\|\mathbf{s}_{ij}(t)\|} = \frac{\mathbf{s}_{ij}(t)}{2R}, \quad (37)$$

$$\hat{q}_{ij}(t) := \frac{\dot{\mathbf{s}}_{ij}(t)}{\|\dot{\mathbf{s}}_{ij}(t)\|} = \frac{\dot{\mathbf{s}}_{ij}(t)}{a_{ij}(t)}, \quad (38)$$

where $\hat{p}_{ij}(t) \cdot \hat{q}_{ij}(t) = 0$ by (17).

To solve the (32) - (35) we will project $\ddot{\mathbf{s}}_{ij}(t)$ onto the contact basis (Definition 3). From (17) we can project $\ddot{\mathbf{s}}_{ij}$ onto \hat{p}_{ij} by

$$\ddot{\mathbf{s}}_{ij}(t) \cdot \mathbf{s}_{ij}(t) = -\dot{\mathbf{s}}_{ij}(t) \cdot \dot{\mathbf{s}}_{ij}(t) = -a_{ij}^2(t). \quad (39)$$

Next, we will solve for the projection of $\ddot{\mathbf{s}}_{ij}$ onto \hat{q}_{ij} as follows: first, integrate this quantity using integration by parts

$$\begin{aligned} \int \ddot{\mathbf{s}}_{ij}(t) \cdot \dot{\mathbf{s}}_{ij}(t) dt &= \dot{\mathbf{s}}_{ij}(t) \cdot \dot{\mathbf{s}}_{ij}(t) \\ &\quad - \int \ddot{\mathbf{s}}_{ij}(t) \cdot \dot{\mathbf{s}}_{ij}(t) dt. \end{aligned}$$

Next, combine the integrals on the left hand side

$$2 \int \ddot{\mathbf{s}}_{ij}(t) \cdot \dot{\mathbf{s}}_{ij}(t) dt = \dot{\mathbf{s}}_{ij}(t) \cdot \dot{\mathbf{s}}_{ij}(t) = a_{ij}^2(t). \quad (40)$$

Finally, take the derivative of both sides, which simplifies to

$$\ddot{\mathbf{s}}_{ij}(t) \cdot \dot{\mathbf{s}}_{ij}(t) = a_{ij}(t) \cdot \dot{a}_{ij}(t). \quad (41)$$

Therefore, the projection of $\ddot{\mathbf{s}}_{ij}$ onto the contact basis is

$$\ddot{\mathbf{s}}_{ij}(t) = \begin{bmatrix} -a_{ij}^2(t) \frac{1}{2R} \\ \dot{a}_{ij}(t) \end{bmatrix}. \quad (42)$$

Finally, we can use (42) to solve for the time derivatives of (37) and (38). First we have

$$\frac{d}{dt} \hat{p}_{ij}(t) = \frac{\dot{\mathbf{s}}_{ij}(t)}{2R} = \frac{a(t)}{2R} \hat{q}_{ij}(t). \quad (43)$$

Then, by the quotient rule,

$$\begin{aligned} \frac{d}{dt} \hat{q}_{ij}(t) &= \frac{\ddot{\mathbf{s}}_{ij}(t) a_{ij}(t) - \dot{\mathbf{s}}_{ij}(t) \dot{a}_{ij}(t)}{a_{ij}^2(t)} \\ &= \frac{a_{ij}(t) \left(-a^2(t) \frac{1}{2R} \hat{p}_{ij}(t) + \dot{a}_{ij}(t) \hat{q}_{ij}(t) \right)}{a_{ij}^2(t)} \\ &\quad - \frac{\dot{\mathbf{s}}_{ij}(t) \dot{a}_{ij}(t)}{a_{ij}^2(t)} \\ &= -\frac{a(t)}{2R} \hat{p}_{ij}(t). \end{aligned} \quad (44)$$

By (6), we may now write $\ddot{\mathbf{s}}_{ij}(t)$ projected on to the contact basis (Definition 3) as

$$\begin{aligned} \ddot{\mathbf{s}}_{ij}(t) &= \mathbf{u}_j(t) - \mathbf{u}_i(t) = -\mathbf{L}_{ij}^v(t) + m_{ij}(t) \mathbf{s}_{ij}(t) \\ &= -\mathbf{L}_{ij}^v(t) \cdot \begin{bmatrix} \hat{p}_{ij}(t) \\ \hat{q}_{ij}(t) \end{bmatrix} + m_{ij}(t) \cdot \begin{bmatrix} 2R \\ 0 \end{bmatrix} \end{aligned} \quad (45)$$

where $m_{ij}(t) = \mu_{ij}(t) + \mu_{ji}(t)$, and $\mathbf{L}_{ij}^x(t) = \lambda_j^x(t) - \lambda_i^x(t)$. Next we substitute (39) and (41) into (45) and rewrite it as a system of scalar equations,

$$\mathbf{L}_{ij}^v(t) \cdot \hat{p}_{ij}(t) = \frac{a_{ij}^2(t)}{2R} + 2R m_{ij}(t), \quad (46)$$

$$\mathbf{L}_{ij}^v(t) \cdot \hat{q}_{ij}(t) = -\dot{a}_{ij}(t). \quad (47)$$

Taking a time derivative yields

$$\dot{\mathbf{L}}_{ij}^v(t) \cdot \hat{p}_{ij}(t) + \mathbf{L}_{ij}^v(t) \cdot \dot{\hat{p}}_{ij}(t) = \frac{a_{ij}(t) \dot{a}_{ij}(t)}{R} + 2R \dot{m}_{ij}(t), \quad (48)$$

$$\dot{\mathbf{L}}_{ij}^v(t) \cdot \hat{q}_{ij}(t) + \mathbf{L}_{ij}^v(t) \cdot \dot{\hat{q}}_{ij}(t) = -\ddot{a}_{ij}(t). \quad (49)$$

Then we substitute (33), (43), and (44) into (48) and (49) which simplifies to

$$\mathbf{L}_{ij}^p(t) \cdot \hat{p}_{ij}(t) = 4R \dot{m}_{ij}(t) - \frac{3}{2R} a_{ij}(t) \dot{a}_{ij}(t) \quad (50)$$

$$\mathbf{L}_{ij}^p(t) \cdot \hat{q}_{ij}(t) = -\dot{a}_{ij}(t). \quad (51)$$

Repeating this process of deriving and substituting on (50) and (51) yields a pair of coupled nonlinear second-order ordinary differential equations,

$$a_{i,j}^4(t) + 32R^4 \ddot{m}_{i,j}(t) = 12R^2 \dot{a}_{i,j}^2(t) + 16R^2 a_{i,j}(t) \ddot{a}_{i,j}(t) + 8R^2 a_{i,j}^2(t) m_{i,j}(t), \quad (52)$$

$$\frac{3}{2R} a_{i,j}^2(t) \dot{a}_{i,j}(t) = 2a_{i,j}(t) \dot{m}_{i,j}(t) + \ddot{a}_{i,j}(t) + 2m_{i,j}(t) \dot{a}_{i,j}(t). \quad (53)$$

Thus, for any constrained trajectory to be energy-optimal it must be a solution of (52) and (53) while also satisfying the boundary conditions (25) and (26). In general this is difficult, as both equations are nonlinear and (53) is third order. However, if we impose that $\dot{a}_{ij} = 0$ and $a_{ij} > 0$, we may simplify and solve (52) and (53) for a candidate optimal trajectory while always satisfying the assumption in Definition 3. This yields

$$a_{ij}^4 + 32R^4 \ddot{m}_{ij}(t) - 8R^2 a_{ij}^2 m_{ij}(t) = 0, \quad (54)$$

$$2a_{ij} \dot{m}_{ij}(t) = 0, \quad (55)$$

with the solution

$$m_{ij}(t) = \frac{a_{ij}^2}{8R^2}. \quad (56)$$

By combining (56) with (33), (34), and (45) we obtain the constrained optimal control input

$$\mathbf{u}_i(t) = \frac{a_{ij}^2}{2R} \hat{p}_{ij}(t) + \mathbf{u}_c(t), \quad (57)$$

$$\mathbf{u}_j(t) = -\frac{a_{ij}^2}{2R} \hat{p}_{ij}(t) + \mathbf{u}_c(t), \quad (58)$$

$$\mathbf{u}_c(t) = \mathbf{c}_1 t + \mathbf{c}_2, \quad (59)$$

where $\mathbf{u}_c(t)$ is the acceleration of the point of contact point between the agents $\mathbf{u}_i(t)$ and $\mathbf{u}_j(t)$ describe the constant-speed orbit of each agent about $\mathbf{u}_c(t)$, and \mathbf{c}_1 and \mathbf{c}_2 are constants of integration. Equations (57) - (59) are solutions to (52) and (53); therefore they constitute locally energy-optimal trajectories.

To generate a final energy-optimal trajectory, each agent will piece together unconstrained and constrained arcs during each trajectory update. In the following section, we present the decentralized strategy used by each agent to generate collision-free and energy-optimal trajectories in real time.

C. Decentralized Trajectory Generation

To generate the trajectory of each agent we will use the following definition of contact intervals..

Definition 4. For each agent $i \in \mathcal{A}$ we define $g \in \mathbb{N}$ contact intervals indexed by $k = 1, 2, \dots, g$. These g intervals must satisfy

$$\tau_i^k \subset [t_0, t_f] \text{ such that}$$

$$\mathcal{V}_i(t_a) = \mathcal{V}_i(t_b) \neq \emptyset \quad \forall t_a, t_b \in \tau_i^k,$$

where for any two intervals $p, q \in \mathbb{N}$, $p \neq q$, we have $t_p < t_q$ for $t_p \in \tau_i^p$ and $t_q \in \tau_i^q$. The contact intervals correspond to the nonzero and non-overlapping intervals of time where $\mathcal{V}_i(t)$ is invariant.

With Definition 4 each agent $i \in \mathcal{A}$ will perform the following steps simultaneously:

- i) Generate an unconstrained trajectory for $t \in [t_0, t_f]$.
- ii) Exchange unconstrained trajectories with its neighbors.
- iii) Calculate $\mathcal{V}_i(t)$.
- iv) Generate a constrained arc for every contact interval (Definition 4).
- v) Piece together all constrained arcs using unconstrained trajectories and continuity conditions.
- vi) Generate initial and final unconstrained arcs to satisfy boundary conditions.
- vii) Generate escape arcs.

The above steps will be performed by all agents simultaneously and repeated with a period of ΔT per our control framework. The details of each step are presented for some agent $i \in \mathcal{A}$ next, but all steps are performed by all agents simultaneously.

i) *Generate a nominal trajectory.* Agent $i \in \mathcal{A}$ generates its unconstrained trajectory by solving (20) - (22). To calculate the flocking error, neighbor information from the previous trajectory, $\mathbf{x}_j(t_f - \Delta T)$, $j \in \mathcal{N}_i(t_0)$ is used.

ii) *Exchange unconstrained trajectories with neighbors.* Each unconstrained trajectory consists of only the eight constants contained in (20) - (22). Therefore, only these coefficients must be communicated between agent $i \in \mathcal{A}$ and its neighbors $j \in \mathcal{N}_i(t_0)$. This happens instantaneously and without error under Assumption 2.

iii) *Calculate $\mathcal{V}_i(t)$.* Agent $i \in \mathcal{A}$ uses the current unconstrained trajectory of agent $j \in \mathcal{N}_i$ to calculate $\mathbf{s}_{ij}(t)$ and determine $\mathcal{V}_i(t)$ by (31). This is used to directly calculate the contact intervals $\tau_i^1, \dots, \tau_i^g$ (Definition 4) as $i \in \mathcal{V}_j(t)$ if and only if $j \in \mathcal{V}_i(t)$.

iv) *Generate constrained arcs.* For each of the $k = 1, 2, \dots, g$ contact intervals agent $i \in \mathcal{A}$ calculates the following parameters for every other agent $j \in \mathcal{V}_i(t)$, $t \in \tau_i^k$.

$$\mathbf{x}_{cg}(t_1^k) = \frac{1}{2} (\mathbf{x}_j(t_1^k) + \mathbf{x}_i(t_1^k)) \quad (60)$$

$$\mathbf{x}_{cg}(t_2^k) = \frac{1}{2} (\mathbf{x}_j(t_2^k) + \mathbf{x}_i(t_2^k)) \quad (61)$$

$$\phi_i(t_1^k) = \text{atan2}(\mathbf{s}_{ij}^y(t_1^k), \mathbf{s}_{ij}^x(t_1^k)) \quad (62)$$

$$\phi_i(t_2^k) = \text{atan2}(\mathbf{s}_{ij}^y(t_2^k), \mathbf{s}_{ij}^x(t_2^k)) \quad (63)$$

$$\psi_i = \frac{\pi}{2} \text{sign}\{(\phi_i(t_2^k) - \phi_i(t_1^k) \bmod 2\pi)\} \quad (64)$$

where $t_1^k = \min\{\tau_i^k\}$ and $t_2^k = \max\{\tau_i^k\}$ are the contact interval limits, $x_{cg}(t_1^k)$ and $x_{cg}(t_2^k)$ define the boundaries for

the constrained arc, $\phi_i(t)$ defines the orientation of $\hat{p}_{ij}(t)$ in the global frame, and ψ_i defines the orientation of $\hat{q}_{ij}(t)$ relative to $\hat{p}_{ij}(t)$. As the relative speed between agents is enforced to be constant, $\phi(t)$ is a linear function over the interval $t \in [t_1^k, t_2^k]$. This is a sufficient number of conditions to completely determine the optimal constrained trajectory of each agent which results from integrating (57) - (59).

v) *Piece together constrained arcs.* With the $g \in \mathbb{N}$ constrained arcs defined, agent $i \in \mathcal{A}$ must piece together each pair of contact intervals, τ_p, τ_q , $q = p + 1$, $0 < p < g$, with unconstrained arcs. This is achieved by recursively applying steps i) - iv) between each of the constrained arcs.

vi) *Generate initial and final unconstrained arcs.* Finally, agent $i \in \mathcal{A}$ must generate two unconstrained arcs, one for the time $t \in [t_0, \min\{\tau_i^1\}]$ and a second for $t \in [\max\{\tau_i^g\}, t_f]$. If either of these unconstrained arcs violate (7) the interval τ_i^1 or τ_i^g must be expanded until no collisions occur. These arcs are allowed to be length zero, which implies agent i may start or end with the collision avoidance constraint active.

vii) *Generate escape arcs.* To further improve performance, agent $i \in \mathcal{A}$ is allowed to *escape* any constrained arc on the interval τ_i^k at some time $t_e \in \tau_i^k$. This is allowed only if the resulting unconstrained arc does not violate (7) and satisfies all interior and boundary conditions. This effectively reduces τ_i^k to the interval $[t_1^k, t_e]$ without affecting $\mathcal{V}_j(\tau_i^k)$ for $j \in \mathcal{V}_i(\tau_i^k)$.

After applying steps i) - vii), agent $i \in \mathcal{A}$ will have generated an energy-optimal trajectory which results in flocking behavior and guarantees safety from inter-agent collisions. What follows is a set of simulation results demonstrating the efficacy of the proposed control algorithm.

IV. SIMULATION RESULTS

To validate our decentralized controller, we developed two sets of simulations. First, we implemented the controller in MATLAB, where the unconstrained and distance-constrained trajectories could be validated on double integrator agents. Next, the controller was applied to a set of AscTec quadrotors in the Gazebo simulation package. The results of this simulation show that our optimal controller generates high-level trajectories which display emergent flocking behavior. These trajectories are also realizable by the dynamics and low-level flight controller of a commercially available quadrotor.

To enhance the performance of the controller, the coefficients in the flocking error function, (11), were normalized such that each component (12) - (14) had a magnitude around 1 during normal operation. These scaling factors are given by

$$w_1 = \frac{k_d}{\|\mathbf{v}_d\|}, \quad w_3 = \frac{k_p}{D^2 N}, \quad w_2 = \frac{k_v}{\|\mathbf{v}_d\|} \quad (65)$$

where k_p, k_v , and k_d are control gains, and are given along with the remaining system parameters in Table I.

A. MATLAB Simulation

We explored two scenarios through simulation in MATLAB. We first initialized two agents such that a collision

Variable	Symbol	Value
Horizon	T	0.4 s
Update Period	ΔT	0.1 s
Position gain	k_p	1.5
Velocity gain 1	k_v	1.0
Velocity gain 2	k_d	3.0

TABLE I

SYSTEM PARAMETERS USED FOR THE MATLAB AND GAZEBO SIMULATIONS.

would occur in the unconstrained case (Figure 2). This result illustrates the collision-avoidance capability of the proposed algorithm. Next we placed 12 agents at feasible initial points randomly within the domain ran the simulation for 30 seconds. The results of this flocking behavior are summarized in Figures 3 and 4.

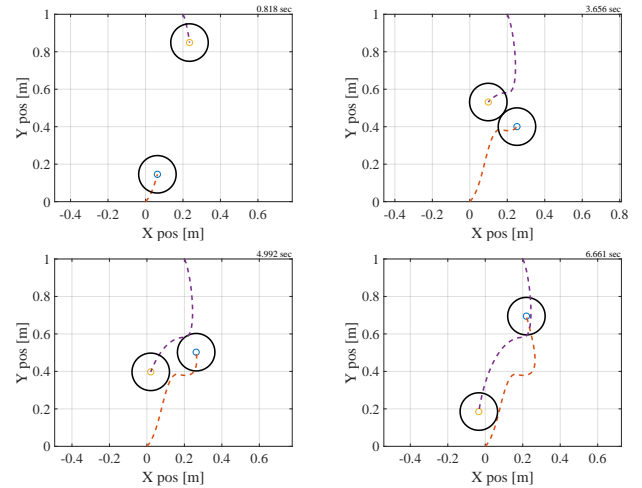


Fig. 2. Numerical simulation for two agents approaching on a colliding trajectory. The agents adjust their speed to contact at a tangent, move past each other, and escape to continue unconstrained.

The results presented in Figures 3 and 4 show that after a short transient period a stable flock is formed. This flock moves in the direction specified by \mathbf{v}_d and begins to cruise at a constant speed around $t = 10$ seconds. This smooth, stable behavior results from each agent following a minimum energy trajectory while forming the flock aggregate.

B. Gazebo Simulation

We performed the second simulation using a *sensing-based approximation* of the derived optimal control algorithm. This approximation is less optimal than the previous case; however, it has the benefits of no communication between the agents and an explicit closed-form solution. The sensing-based approach for agent $i \in \mathcal{A}$ approximates (29) as

$$\mathbf{p}_i(t_f) = \sum_{j \in \mathcal{N}_i} \mathbf{p}_j(t_0) + \frac{\mathbf{a}_i}{2w_3 \sum_j (\|\mathbf{s}_{ij}(t_0)\| - D)}, \quad (66)$$

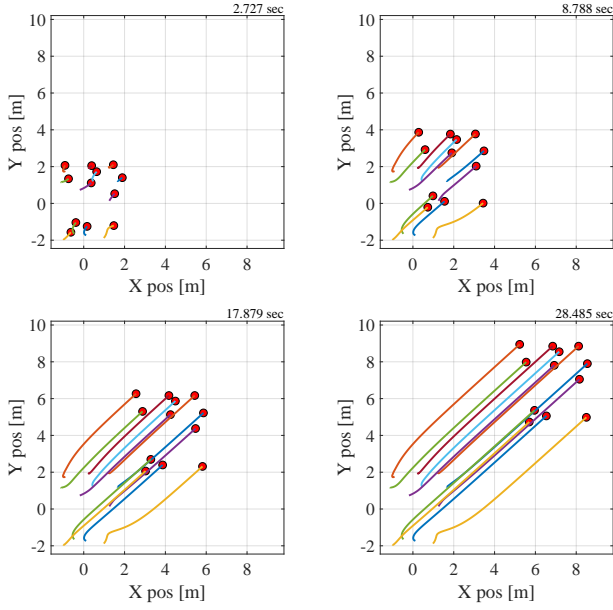


Fig. 3. Flocking behavior for 12 agents simulated in MATLAB. Agents initially form an aggregate before flocking to the northeast.

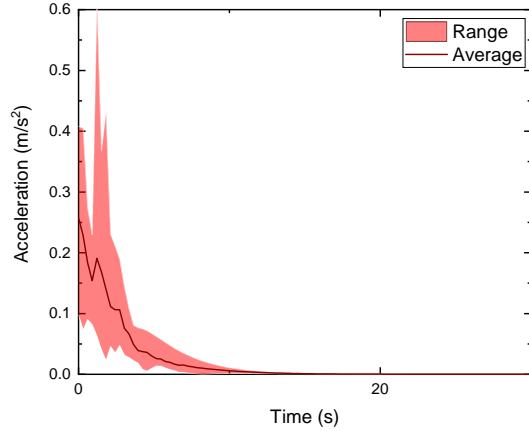


Fig. 4. A plot of maximum and average acceleration magnitude vs time for the flocking behavior in MATLAB (Figure 3). The initial spike comes from the transient formation of the flock, and the energy consumed by each agent quickly drops to zero.

where $\mathbf{p}_j(t_0)$, $j \in \mathcal{N}_i(t_0)$ must only be sensed by agent i . The emerging quadrotor behavior still resembled flocking, as can be seen in Figure 5.

These simulations were carried out in Gazebo using the RotorS package [29] and six AscTec Hummingbirds operating in a horizontal plane. The parameters used for each simulation were: $D = 0.25$ m, $\mathbf{v}_d = (2.5, 0)$ m/s, and $h = 4.5$ m. The results of these simulations are visualized in Figures 5 and 6

The Gazebo simulation validates the asymptotic reduction in energy consumption seen in Figure 4; even for agents with significantly more complex dynamics, i.e., drones. Additionally, the sensing-only approximation (66) has a negligible impact on the global structure of the flock and rate of energy

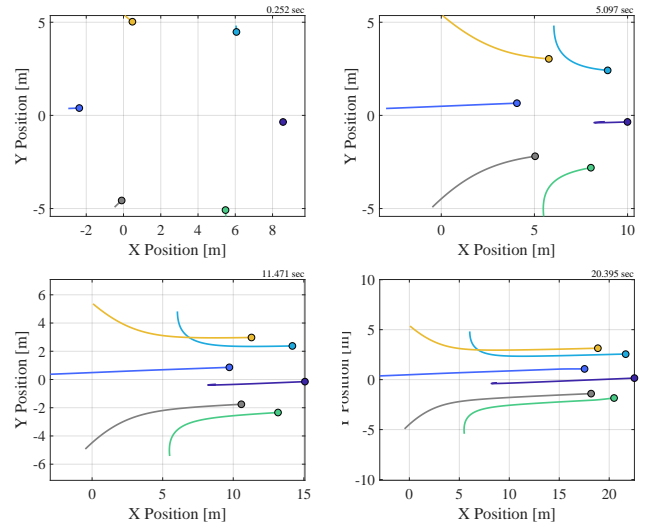


Fig. 5. Gazebo simulation with six agents spaced in a hexagonal formation. The agents initially coalesce into a hexagonal pattern before flocking along the direction of \mathbf{v}_d . The flock naturally forms a hexagon near the end of the simulation.

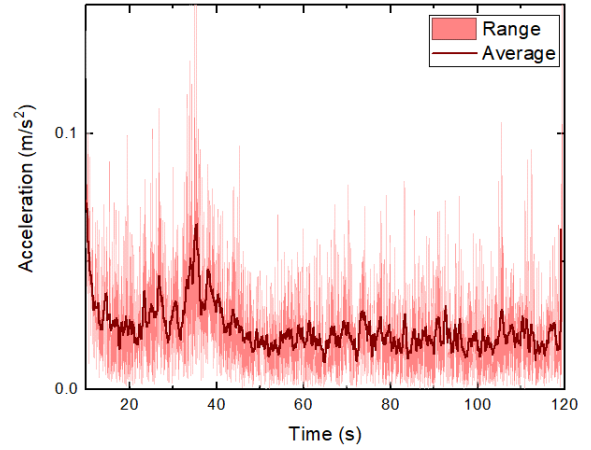


Fig. 6. Time series of the average and maximum acceleration magnitude for the six drones in Fig. 5. The acceleration limits and average were smoothed with a moving average with windows of 51 and 510 ms, respectively, for readability. An initial 10 second liftoff time has been omitted from the figure.

consumption in this scenario.

C. Observed Emergent Behavior

The desired emergent flocking behavior resulting from the selection of $\Phi(t)$ (Definition 2) can be observed in Figures 3 and 5. By varying the scaling factors in the flocking error (Definition 2), the different constituent behaviors, i.e., velocity matching, velocity control, and aggregation, may come to dominate. The selection of these scaling factors has a profound impact on the stability, oscillation, and convergence of the flock.

The selection of the horizon, h , relative to the desired distance, D , also has a significant effect on the structure of the flock. Allowing $h > 2D$ may lead to flock implosion,

as agents form tight clusters and activate their collision avoidance constraints. This is a result of the L2 norm in ϕ_p , (14), which causes attractive behavior to dominate any repulsive effect if there are any neighbors farther than $D + 2R < h$.

An unintended behavior was the formation of stable 2-cliques and 3-cliques within and outside the flock. This is a consequence of the flock centroid attractor, (13) and (14), which only activates for isolated agents. This behavior may also occur in vector field methods, and the formation of stable cliques is entirely dependent on the initial state of the flock.

V. CONCLUSION

In this paper, we proposed an optimal control approach to realize flocking behavior in a group of cooperative agents. We presented the optimal trajectory in the form of a boundary value problem and provided a candidate optimal solution. We then verified the efficacy of the proposed controller via simulation with two cases. First, the algorithm was simulated in MATLAB to show the emergence of flocking behavior. We then introduced a sensing only approximation to the controller in Gazebo, which resulted in qualitatively similar flocking behavior.

Future areas of research include extending the obstacle avoidance constraint to include terrain and mobile obstacles, redefining the aggregation function to use a local description of flocking, and testing the optimal control algorithm on physical hardware in the University of Delaware Scaled Smart City.

ACKNOWLEDGMENTS

The authors would like to thank Michael Dorothy at Combat Capabilities Development Command, Army Research Laboratory, for the insightful discussions and remarks.

REFERENCES

- [1] A. A. Malikopoulos, "A duality framework for stochastic optimal control of complex systems," *IEEE Transactions on Automatic Control*, vol. 61, no. 10, pp. 2756–2765, 2016.
- [2] —, "Centralized stochastic optimal control of complex systems," in *Proceedings of the 2015 European Control Conference*, 2015, pp. 721–726.
- [3] —, "Equilibrium Control Policies for Markov Chains," in *50th IEEE Conference on Decision and Control and European Control Conference*, 2011, pp. 7093–7098.
- [4] A. A. Malikopoulos, V. Maroulas, and J. Xiong, "A multiobjective optimization framework for stochastic control of complex systems," in *Proceedings of the 2015 American Control Conference*, 2015, pp. 4263–4268.
- [5] H. Oh, A. R. Shirazi, C. Sun, and Y. Jin, "Bio-inspired self-organising multi-robot pattern formation: A review," *Robotics and Autonomous Systems*, vol. 91, pp. 83–100, 2017.
- [6] A. A. Malikopoulos, C. G. Cassandras, and Y. J. Zhang, "A decentralized energy-optimal control framework for connected automated vehicles at signal-free intersections," *Automatica*, vol. 93, no. April, pp. 244–256, 2018.
- [7] Q. Lindsey, D. Mellinger, and V. Kumar, "Construction with quadrotor teams," *Autonomous Robots*, 2012.
- [8] J. Cortes, "Global formation-shape stabilization of relative sensing networks," in *Proceedings of the American Control Conference*, 2009.
- [9] C. W. Reynolds, "Flocks, herds and schools: A distributed behavioral model," *Computer Graphics*, vol. 21, no. 4, pp. 25–34, 1987.
- [10] R. Olfati-Saber, "Flocking for multi-agent dynamic systems: Algorithms and theory," *IEEE Transactions on Automatic Control*, vol. 51, no. 3, pp. 401–420, 3 2006.
- [11] A. Barve and M. J. Nene, "Survey of Flocking Algorithms in Multi-agent Systems," *International Journal of Computer Science*, vol. 19, no. 6, pp. 110–117, 2013.
- [12] S.-J. Chung, A. Paranjape, P. Dames, S. Shen, and V. Kumar, "A Survey on Aerial Swarm Robotics," *IEEE Transactions on Robotics*, vol. 34, no. 4, p. 837/855, 2018.
- [13] K.-K. Oh, M.-C. Park, and H.-S. Ahn, "A survey of multi-agent formation control," *Automatica*, vol. 53, pp. 424–440, 2015.
- [14] G. Vásárhelyi, C. Virágh, G. Somorjai, T. Nepusz, A. E. Eiben, and T. Vicsek, "Optimized flocking of autonomous drones in confined environments," *Science Robotics*, vol. 3, no. 20, 2018. [Online]. Available: <http://robotics.sciencemag.org/>
- [15] H. G. Tanner, A. Jadbabaie, and G. J. Pappas, "Flocking in fixed and switching networks," *IEEE Transactions on Automatic Control*, vol. 52, no. 5, pp. 863–868, 2007.
- [16] H. X. Egerstedt, "Formation Constrained Multi-Agent Control," *IEEE Transactions on Robotics and Automation*, vol. 17, no. 6, pp. 947–951, 2001.
- [17] G. A. S. Pereira, M. F. M. Campos, and V. Kumar, "Decentralized Algorithms for Multi-Robot Manipulation via Caging," *The International Journal of Robotics Research*, vol. 23, no. 7, pp. 783–795, 2004.
- [18] C. E. Luis and A. P. Schoellig, "Trajectory Generation for Multiagent Point-To-Point Transitions via Distributed Model Predictive Control," *IEEE Robotics and Automation Letters*, vol. 4, no. 2, pp. 375–382, 4 2019.
- [19] D. Morgan, G. P. Subramanian, S.-J. Chung, and F. Y. Hadaegh, "Swarm assignment and trajectory optimization using variable-swarm, distributed auction assignment and sequential convex programming," *International Journal of Robotics Research*, vol. 35, no. 10, pp. 1261–1285, 2016.
- [20] M. Turpin, N. Michael, and V. Kumar, "CAPT: Concurrent assignment and planning of trajectories for multiple robots," *International Journal of Robotics Research*, vol. 33, no. 1, pp. 98–112, 2014.
- [21] M. Turpin, K. Mohta, N. Michael, and V. Kumar, "Goal Assignment and Trajectory Planning for Large Teams of Aerial Robots," *Proceedings of Robotics: Science and Systems*, vol. 37, pp. 401–415, 2013.
- [22] L. E. Beaver and A. A. Malikopoulos, "A Decentralized Control Framework for Energy-Optimal Goal Assignment and Trajectory Generation," in *Proceedings of the 2019 Conference on Decision and Control (to appear)*, Nice, FR, 2019.
- [23] M. Egerstedt, J. N. Pauli, G. Notomista, and S. Hutchinson, "Robot ecology: Constraint-based control design for long duration autonomy," pp. 1–7, 1 2018.
- [24] S. A. Quintero, G. E. Collins, and J. P. Hespanha, "Flocking with fixed-wing UAVs for distributed sensing: A stochastic optimal control approach," in *Proceedings of the American Control Conference*, 2013, pp. 2025–2031.
- [25] H. T. Zhang, Z. Cheng, G. Chen, and C. Li, "Model predictive flocking control for second-order multi-agent systems with input constraints," *IEEE Transactions on Circuits and Systems I: Regular Papers*, vol. 62, no. 6, pp. 1599–1606, 6 2015.
- [26] V. Gómez, S. Thijssen, A. Symington, S. Hailes, and H. J. Kappen, "Real-Time Stochastic Optimal Control for Multi-agent Quadrotor Swarms," in *26th International Conference on Automated Planning and Scheduling*. London: AAAI Press, 2016, p. 17.
- [27] Y. Hu, J. Zhan, and X. Li, "Self-triggered distributed model predictive control for flocking of multi-agent systems," *IET Control Theory & Applications*, vol. 12, no. 18, pp. 2441–2448, 12 2018.
- [28] A. E. J. Bryson and Y.-C. Ho, *Applied Optimal Control: Optimization, Estimation, and Control*. John Wiley and Sons, 1975.
- [29] F. Furrer, M. Burri, M. Achtelik, and R. Siegwart, "RotorS—A Modular Gazebo MAV Simulator Framework," in *Robot Operating System (ROS): The Complete Reference (Volume 1)*, A. Koubaa, Ed. Cham: Springer International Publishing, 2016, pp. 595–625.